2016 IEEE International Conference on Robotics and Automation (ICRA)
Stockholm, Sweden, May 16-21, 2016

Magnetic Microrobots with Addressable Shape Control

Hen-Wei Huang, Mahmut Selman Sakar, Katharina Riederer, Naveen Shamsudhin, Andrew Petruska, Salvador Pané, and Bradley J. Nelson

Abstract—**Shape shifting soft microrobots are generated from self-folding hydrogel bilayer structures. The folding conditions are analyzed to develop an optimal strategy for producing desired three-dimensional shapes. We present two different methods for programming magnetization in these microrobots that are variant and invariant to folding. The microrobots can be navigated through user-defined trajectories using rotating magnetic fields, and the morphing in response to temperature changes can be tuned for adaptive behavior. On-demand modulation of the mobility of individual microrobots is demonstrated by morphing their shape using selective near infrared light (NIR) exposure.**

I. Introduction

Recent work has shown that wirelessly controlled self-shaping hydrogel devices have potential applications for minimally invasive interventions [1, 2]. Compared to other actuation methods, magnetic manipulation provides more degrees of freedom (DOFs) for locomotion [3], which are required to perform dexterous manipulation with high precision for medical, biological, and manufacturing applications. A hollow 3D object such as a capsule or tube provides a large surface-area-to-volume ratio and carrying space for therapeutic agents. High payload capacity is desirable for cell encapsulation and transportation [4], targeted drug delivery [5] and sustained drug release [6]. Self-folding films are able to form different 3D structures through a template-free fabrication process that is highly compatible with standard MEMS batch processing. Forming films from stimuli responsive materials enables the reconfiguration of their morphologies in response to external stimuli [7]. Depending on the material choice, this shape change can be triggered by a variety of different signals including magnetic and light waves [2, 8].

We fabricated self-folding microrobots with a hollow cylindrical shape by patterning hydrogel bilayers using conventional 2D photolithography. A two steps process was used to couple a thermally responsive hydrogel nanocomposite with a thin inactive layer. Different swelling behaviors between these layers cause an inhomogeneous swelling/shrinking, which leads to folding of the planar structure into a 3D functional micromachine. Under NIR light exposure, the structures are heat up and unfold. When the temperature exceeds a certain threshold, they fold into a different shape. The overall concept is summarized in Fig. 1.

The swelling characteristic of hydrogel is due to the ability to retain fluid in its polymer network. The magnetization and folding conditions of self-folding microrobots are both related to the swelling properties of the responsive layer. In order to obtain desired body plans with programmed magnetization,

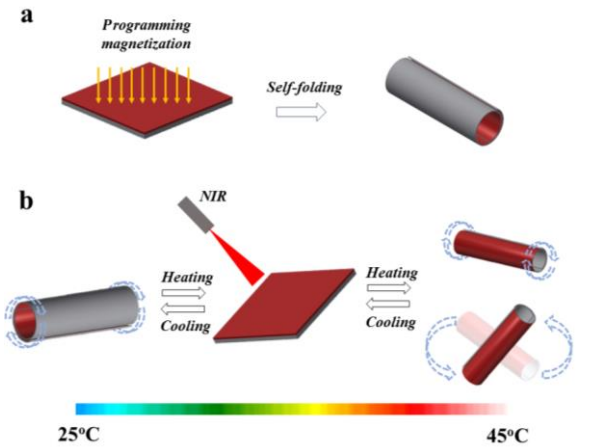

Figure 1. (a) Programmable magnetization and folding of hydrogel bilayers to generate magnetically controllable microrobots. (b) Shape switching concept for soft microrobots by increasing temperature using near infrared light exposure.

the folding conditions and shape transformation must be well understood. Defects in the folding process will result in deviations in magnetic anisotropy and locomotion gaits accordingly. Magnetic anisotropy can be programmed in polymer-based actuators [9] and the same method has been recently used to program the magnetic anisotropy of helical structures and demonstrate wobble-free corkscrew motion [10]. In polymeric devices, the shape of the structures does not change after polymerization. However, the alignment of magnetic nanoparticles embedded inside the self-folding hydrogel bilayers must be tailored considering the final shape and the propulsion mechanism of the functional microrobot.

In this work, the swelling properties of the hydrogel bilayers were tuned to obtain desirable folding while encoding strong enough magnetization for actuation. There are two methods for setting the direction of magnetization of self-folding microrobots. The first one results in fold-invariant magnetization. This technique ensures that the magnetization is always aligned in the radial direction, even if the folding conditions are imperfect. The second one results in folding-variant magnetization in which magnetization can be reprogrammed by morphing the shapes. This enables microrobots to switch between different propulsion mechanisms. Finally, we demonstrate that individual microrobots can be selectively addressed by NIR light and activated for shape transformation. NIR exposure introduces high precision addressing of individual microrobots and the use of shape as an extra degree of freedom. Multi agent control can thus be realized for accomplishing collective tasks.

The authors are with the Institute of Robotics and Intelligent Systems, ETH Zurich, 8092, Zurich, Switzerland. Email: hhuang@ethz.ch

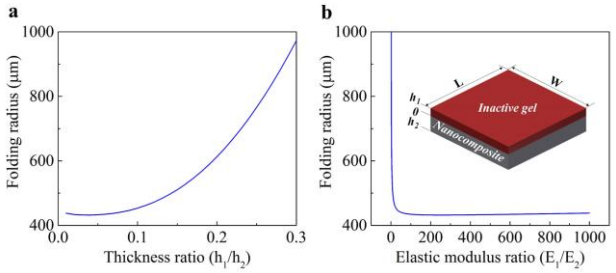

Figure 2. Predicted folding radius of hydrogel bilayers. Folding radius versus (a) the thickness ratio of inactive and nanocomposite layers and (b) the elastic modulus ratio of inactive and nanocomposite layers.

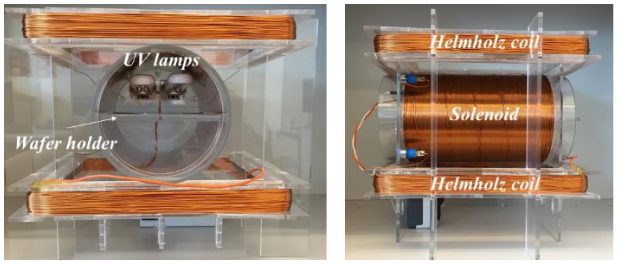

Figure 3. The setup for programming the magnetization of self-folding microrobots.

II. Materials and Methods

A. Folding Conditions of Hydrogel Bilayers

Hydrogel microrobots are composed of two different layers, an inactive layer (polyethylenglycol diacrylate, PEGDA) that is insensitive to changes in temperature and a responsive nanocomposite layer (N-Isopropylacrylamide, NIPAAm) with temperature dependent swelling. The magnetic nanoparticles are incorporated into the responsive layer. A modified mathematic model based on Timoshenko bimorph beam theory [9] can be used to estimate the folding radius of hydrogel bilayers.

$$R = \frac{(h_1+h_2)\left(8(1+m)^2+(1+m\eta)(m^2+\frac{1}{m\eta})\right)}{6\varepsilon(1+m)^2} \qquad (1)$$

where ε is the difference in expansion coefficient between the inactive layer and nanocomposite layer, h_1 is the thickness of the inactive layer, h_2 is the thickness of the nanocomposite, η and m are the ratio between the two layers of the elastic modulus and thickness, respectively. The analytical model suggests that larger differences in the expansion coefficient, lower thickness ratio and higher ratio of the elastic modulus give rise to a smaller folding radius (Fig. 2). To obtain a small folding radius, a thickness ratio of 0.1 was used in this work. When the elastic modulus ratio is higher than a certain value (η=100), there is no significant difference in folding radius (Fig. 2b). A schematic geometry of the hydrogel bilayer plate is shown inside Fig. 2b. The aspect ratio (length to width, L/W) of the hydrogel bilayer was set to 1.1 to control the folding direction. Because of the edge effects in bilayer structures, the bilayers usually fold along the long side [10]. In this work, the mechanical properties of the inactive layer were kept constant. Various folding conditions of self-folded hydrogel bilayers were obtained by varying the swelling properties of the nanocomposite layer.

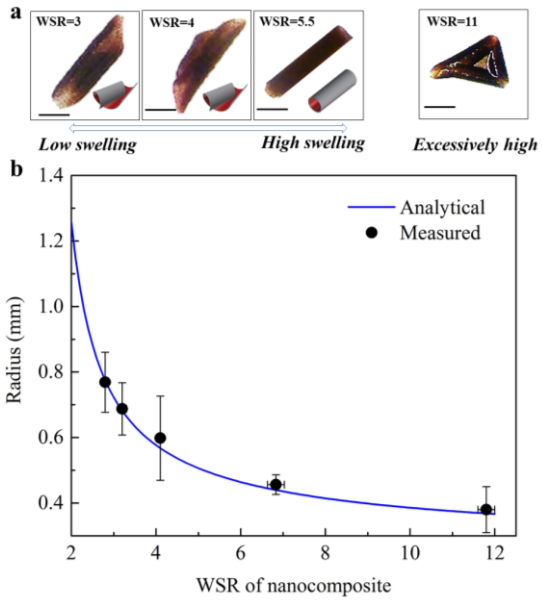

Figure 4. (a) Optical images of various folding conditions of hydrogel bilayers. (b) The measured and estimated folding radius of cylindrical tubes composed of different WSR of nanocomposite at 22ºC. The scale bars are 1 mm.

B. Experimental Setup

The setup to program the magnetization by aligning the embedded magnetic nanoparticles (MNPs) is composed of one solenoid in horizontal direction, one pair of Helmholtz coils in vertical direction, and one pair of UV lamps (Lightning Enterprises, US) integrated inside the solenoid (Fig. 3). The maximum intensity of generated uniform magnetic field governed by each coil is 10 mT in the workspace. Five DOF locomotion of the self-folding microrobots can be achieved by using an eight-coil electromagnetic manipulation system (Octomag) [3]. An NIR laser source (wavelength 808 nm, 1.5 W, SLOC lasers, China) is used to heat up the microrobots and modulate their shape. The system is capable of generating uniform magnetic fields up to 40 mT and magnetic field gradients up to 1 T/m. A top camera observes the scene and image processing detects the position and orientation of the self-folding microrobot and provides feedback for the visual control system. Details of the visual control system is described in [11]. All the experiments are performed in a glass Petri dish placed in the middle of the workspace, filled with deionized water.

C. Methods for Analyzing Hydrogel Nanocomposite

Temperature dependent weight swelling ratio (WSR) of the thermoresponsive nanocomposites and the inactive gel were measured using both gravimetric and imaging methods. Both single inactive layer and nanocomposite layer were produced individually and incubated in a water bath (Julabo, Germany) at several temperatures between 25˚C and 55˚C. Every hour the samples were removed from the water, residual surface water was carefully wiped away, and the weight was recorded.

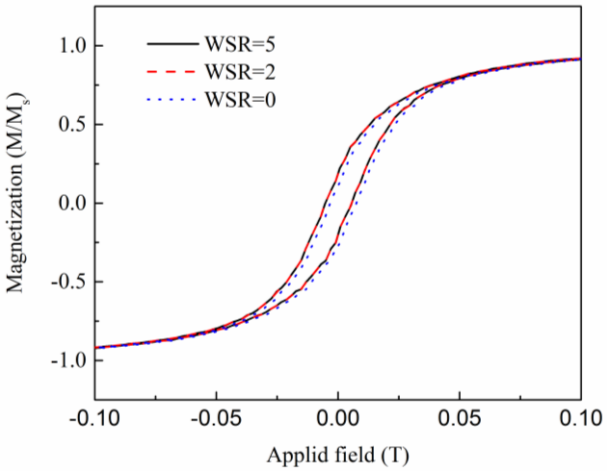

Figure 5. Magnetic properties of nanocomposites with different WSR.

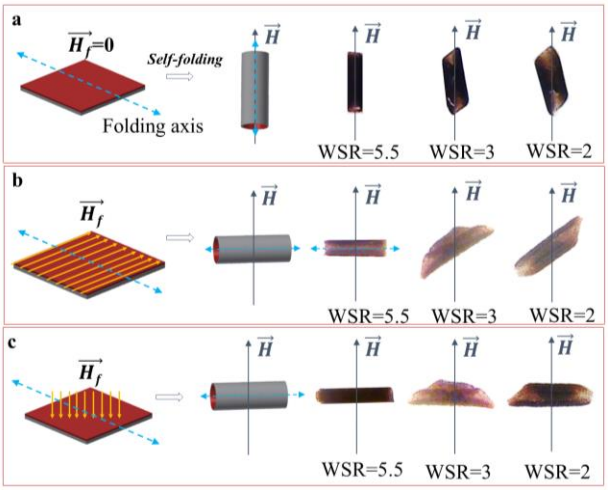

Figure 6. (a) In the absence of particle alignment, the magnetic easy axis is governed by the anisotropic shape. (b) Fold-variant magnetization of bilayers with horizontally aligned MNPs (c) Folding invariant magnetization of bilayers with MNPs aligned out of plane. The blue dash line represents the predicted folding axis of hydrogel bilayers and the yellow solid line represents the applied magnetic field for aligning particles and programming magnetization.

The equilibrium WSR at each temperature was defined as WSR $= (m_s - m_d)/m_d$, where m_s *and* m_d are the mass of the fully swollen and fully dried hydrogel, respectively. Magnetic hysteresis loops of the magnetic nanocomposites with different WSR embedded with 5 vol% of 30 nm Fe_3O_4 were measured at the temperature of 302.3 K by vibratory sample magnetometer (VSM, Oxford Instruments 1.2, and UK) by applying a magnetic field in the range of -1 T to 1 T.

III. Results and Discussions

A. Analysis of the Folding Radius of the Microrobots

The folding conditions of hydrogel bilayers are determined by the difference in swelling properties between two layers. Relatively low WSR of the hydrogel nanocomposites results in small expansion coefficient and large elastic modulus, causing the hydrogel bilayers to fold along the diagonal axis. Relatively high WSR of nanocomposites causes a large difference in hydration between the center part and corner part of the device, resulting in overfolding (see Fig. 4a). There is an optimal range of WSRs that results in appropriate expansion coefficient and elastic modulus to give rise to the desired folding shapes. Fig. 4b shows that the measured radius (outer radius of cylindrical tubes) of the hydrogel bilayers was inversely proportional to the WSR of nanocomposite. By measuring the expansion coefficient and elastic modulus of hydrogel layers, the folding radius can be calculated from equation (1). The calculated values closely follow the measurements. Thus, the proposed analytical model correctly predicts the self-folding radius of the microrobots.

B. Analysis of Magnetization of the Microrobots

We prepared nanocomposite sheets with different WSR by varying the concentration of the cross-linker and keeping the mass of the magnetic particles constant. With increasing WSR, structures absorb more water and the relative mass of magnetic material in the final swollen state decreases. Fig. 5 shows the magnetic properties of the nanocomposite layer with different swelling properties. The overall magnetization of the sheets does not change with WSR as magnetization of these structures primarily depends on the amount and distribution of magnetic material. Therefore, considering the optimal folding conditions described in the previous section, we chose WSR=5 for building our microrobots.

The magnetic easy axis of microrobots, on the other hand, depends on the shape of the folded state. The magnetic easy axis of programmed self-folding microrobots is shown in Fig. 6. In the absence of a particle alignment process, the 3D shape of the microrobots determines the magnetic anisotropy, which is along the long axis of cylinders (Fig. 6a). By aligning the embedded MNPs in horizontal direction and perpendicular to the predicted self-folding axis, the magnetic easy axis of self-folding microrobots changed with the folding conditions. Fig. 6b shows that the magnetic easy axis of a self-folding tube with a desirable folding shape is perpendicular to the self-folding axis as predicted. However, the tubes with undesirable folding conditions have misalignment between their folding axis and their magnetic easy axis. In order to prevent defects in the folded shape resulting in misaligned magnetization, a folding invariant magnetization was introduced in Fig. 6c. By aligning the MNPs in vertical direction (out of plane), the self-folding behavior transformed the out of plane magnetization of a planar sheet to the radial axis of self-folding microrobots. Due to the cylindrical symmetry of magnetization, the self-folding microrobots were able to perform rolling motion even with poor folding conditions.

C. Analysis of Thermal Response of the Microrobots

Bilayers composed of thermally responsive NIPAAm hydrogel have the ability to continuously transform their shapes in response to temperature changes. This morphing behavior will continue until reaching a critical threshold, which is 42˚C for our microrobots. Increasing the temperature beyond this point makes the hydrogel more hydrophobic and dehydrated. The inactive gel is insensitive to temperature variations. Increasing the temperature decreases the difference

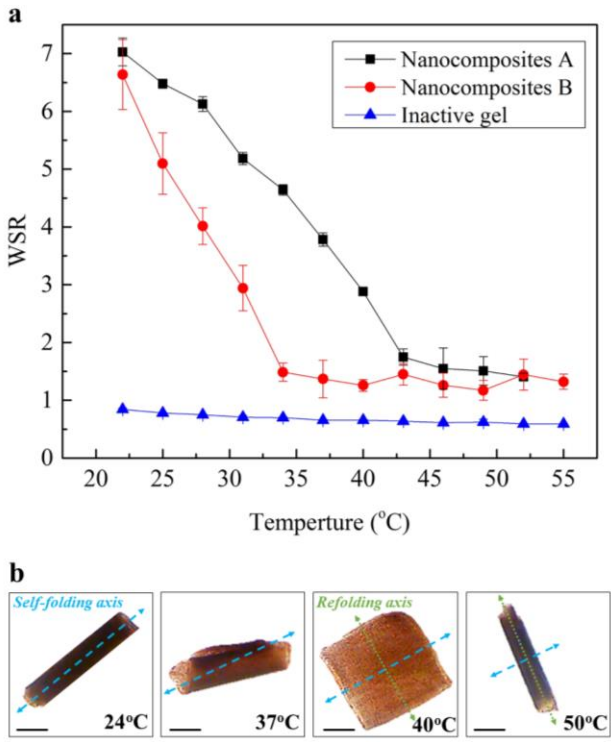

Figure 7. Thermal responsive behavior of hydrogel bilayers. (a) Optical images of the hydrogel bilayer at different temperatures. (b) Analysis of the thermal response of the nanocomposite layer and inactive layer. The folding states of microrobots at different temperature values. The scale bars are 1 mm.

in WSR between the inactive gel and the thermal responsive nanocomposite and the self-folding behavior was recovered. The radius of the microrobot during unfolding behavior increases due to the decrease of the difference in WSR between the two layers. The temperature values the nanocomposite responds to can be adjusted by tuning the ratio of hydrophilic/hydrophobic monomers to NIPAAm hydrogel. At the same temperature value, microrobots with different compositions can transform into different 3D shapes. We prepared two different compositions to demonstrate this feature. Nanocomposite A has a hydrophilic monomer which makes the substrate respond to a larger range of temperature values compared to the layer prepared from nanocomposite B which has no monomer incorporated (see Fig. 7a). By measuring the mechanical properties of the individual layers of hydrogel bilayer at different temperature values and using (1), we can predict the evolution of the radius of the cylinders during unfolding.

Optical images of self-folding microrobots at different temperature values are shown in Fig. 7b. The continuous shape transformation is shown in supporting video. The microrobots unfolded from a tubular shape to an open planar sheet in response to a rise in temperature from 24˚C to 40˚C. Further increase in the temperature initiates a refolding pattern in the opposite direction around the perpendicular axis. This refolding behavior is due to the isotropic shrinking of the nanocomposite layer. When the temperature is increased, the nanocomposite layer shrinks in all directions, which causes it to unfold and then to refold in the opposite direction. The microrobot with folding variant magnetization is able to switch its magnetic easy axis between the short axis and long axis by switching its folding axis. This transformation of shape leads to a switch between rolling and tumbling motion. Fold-invariant magnetization concept can be used to develop robust microrobots that are insensitive to temperature variations.

D. Analysis of Motion of the Microrobots

The microrobot is subjected to an externally applied magnetic field H with a flux density $B = \mu_0 H$, where μ_0 is the permeability of vacuum. The torque that acts on the microrobot can be defined as

$$\tau = VM \times B \qquad (2)$$

where M is the volume magnetization in [A/m] of the object of volume V.

The force acting on the microrobot is described as

$$F = V(M \cdot \nabla)B \qquad (3)$$

Due to the design of the microrobot and the method of actuation (i.e., a rotating magnetic field induces a forward velocity), the system is limited to non-holonomic motion, corresponding to classical unicycle mobile microrobots.

When the microrobot translates and rotates near a surface, it experiences a drag force and drag torque from fluid. Both the drag force and drag torque acting on the microrobot can be estimated by assuming that the microrobot is a solid circular cylinder in a low Reynolds number flow perpendicular to its long axis. Analytical models for the drag force and torque acting on a cylinder in open flow can be found in [12] and [13], respectively. In the case of the self-folding microrobot motion is executed in a confined space close to a wall.

Per unit length of the cylinder (L) the drag force is then defined as [14]

$$F_d/L = \frac{-4\pi\mu_d U}{log2k+\left(\frac{k}{2}\right)^2} \qquad (4)$$

where $k = r_c/d_c$, μ_d is the fluid's dynamic viscosity and U is the relative velocity between the fluid and the microrobot. The parameters corresponding to the wall interaction are the radius of the cylinder (r_c) and the distance between the center of the microrobot and the wall (d_c). The drag torque per L of a cylinder rotating close to a wall is given by [15]

$$\tau_d/L = \frac{4\pi\mu_d\omega r_c^2}{\sqrt{1-k^2}} \qquad (5)$$

As the microrobot contacts the wall ($k = 1$), the surface friction force ($\mu_f \cdot F_v$) will dominate the drag force and drag torque on the microrobot, where the μ_f is coefficient of friction. When the microrobot moves near a surface as shown in Fig. 8, the drag force from the wall causes a difference in velocity of the microrobot between the top (U_T) and bottom

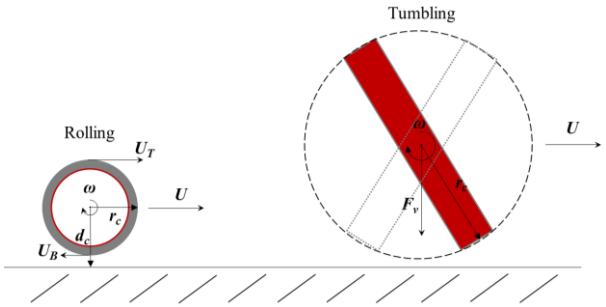

Figure 8. Free body diagram of the microrobot rolling and tumbling on a surface.

(U_B) of the cylinder that induces the forward velocity U. Compared to rolling motion, tumbling motion is subjected to a larger drag force and torque from the fluid due to the larger rotating radius. Tumbling motion must also overcome the additional torque from the volumetric vertical force $\tau_v = \overrightarrow{F_v} \times \overrightarrow{r_c}$, where F_v is the combination of gravitational force and buoyancy from the fluid. By transforming the microrobots with shape variant magnetization, we can program a switch between tumbling and rolling motion. Due to the slip of the microrobot $U < r_c\omega$ at high rotating frequency, which can be written as $U = \mu_s r_c \omega$, where $0 < \mu_s \leq 1$ is the slip coefficient, which depends on the viscosity of the liquid as well as the characteristics of the surfaces of the microrobot and the substrate (see Fig. 8).

D. Adaptive Motion by Tuning Temperature Response

The shape of the microrobots governs the response to the magnetic input due to hydrodynamic forces. As a result, the mobility of shape shifting microrobots can be adapted to different complex environments. Fig. 9 shows how the hydrodynamic shape affects the motion of the microrobots to the applied magnetic field (see supporting video). We engineered two microrobots with different thermal response using the nanocomposite A and nanocomposite B that was described in Fig. 7. They were placed in a warm water bath with a temperature of 40˚C. While the increase in temperature led to the unfolding of first prototype, the second microrobot unfolded and refolded into a tube. The refolded tube was able to roll on the surface in response to a rotating magnetic field. However, the microrobot with the planar geometry has to overcome a significantly higher fluidic drag to be able to rotate on the surface. Fig. 9 shows that the open plate was unable to be manipulated by the 10 mT rotating magnetic field, while the refolded tube can successfully move along the predefined route.

E. Addressable Shape Control

NIR light can be used as a spatiotemporally controlled external signal to trigger selective heating of magnetic nanocomposites [16]. The focused light beam allows us to heat up individual microrobots and reversibly modulate their shape. To demonstrate addressable shape control, we placed four self-folded tubular microrobots in close vicinity and targeted individual microrobots using a NIR laser. The exposed microrobots went through an unfolding and refolding process and recovered their initial shape after the NIR laser was turned off (Fig. 10a). The NIR laser dot was adjusted to be

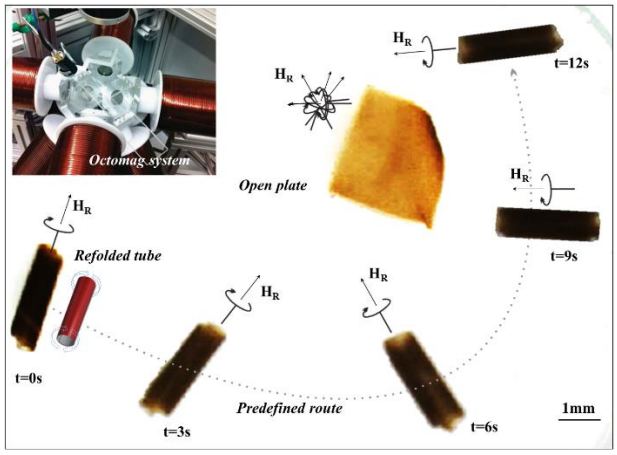

Figure 9. Manipulation of two self-folding microrobots with different dynamic shapes by applying rotating magnetic fields with a pre-defined route. The environment is 40˚C DI water. The field intensity is 10 mT and the frequency is 1 Hz.

the same size as the microrobots to ensure selective exposure. The NIR light exposure can be integrated with magnetic manipulation. To demonstrate on-demand shape change on mobile microrobots, we optically stimulated a microrobot rolling on the surface (Fig. 10b). The microrobot was subjected to the NIR light for five seconds, which triggered the shape transformation from self-folded tube to refolded tube. After the laser is turned off, the temperature of the microrobot goes down due to thermal diffusion and transforms back to the original shape. During the shape transformation process, the microrobots unfold into a plate and stop moving. Once the microrobot recovered its original shape and it started to follow the external magnetic field again.

The forward velocity of the microrobots is proportional to the rotating radius and frequency ($U = \mu_s r_c \omega$). As mentioned before, the folding radius of self-folding microrobots vary with temperature variations. By tuning the radius of microrobots, multiple microrobots can be differentially controlled by global magnetic fields. NIR exposure introduces high precision addressing and using shape as an extra degree of freedom; multi agent control can be realized for accomplishing collective tasks. In the supporting video, we show that two microrobots with the same folding conditions rolled on the surface. The speed of the microrobots can be individually increased upon NIR exposure. An exposure to laser light generates enlargement of the radius of the targeted microrobot, and leads to an increase in forward velocity accordingly. The microrobots exposed to NIR for a long enough period (> five seconds) experienced a reversible unfolding and refolding process. During the unfolding step, the microrobots can no longer follow the magnetic field, which temporarily disables their motion.

The self-folding microrobots can react to the environmental variations and automatically adjust their shapes to perform specific applications in the most efficient way. For instance, self-folding tubes manipulated by rotating magnetic fields can autonomously change their shapes in response to a change in temperature and stop moving to perform targeted interventions (i.e. drug delivery) without feedback from the external control system. The temperature response of the hydrogels can be adjusted by modulating their composition as

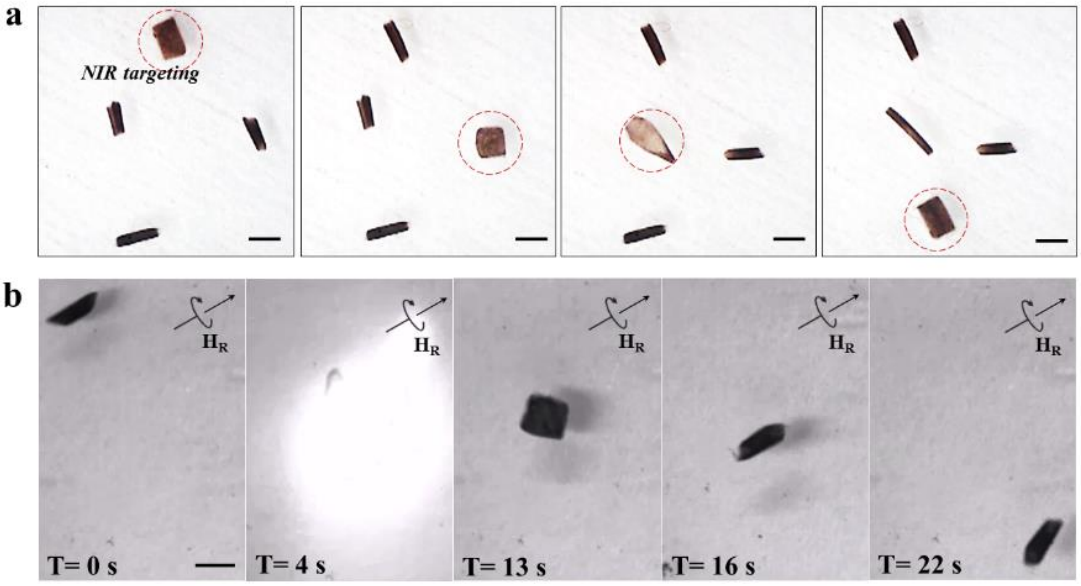

Figure 10. (a) Selective NIR targeting the microrobots. (b) Dynamically modulating the shape of the microrobots. The images are frames from the supporting video. The scale bars are 1 mm.

shown in Fig. 7. By using different stimuli responsive hydrogels [17], the shape transformation of self-folding microrobots could be triggered by different external signals.

IV. Conclusion

In this work, we present a transformable microrobot based on thermally responsive hydrogel bilayers. Different methods for programming magnetization of the microrobots undergoing multiple shape transformations are provided. We studied the relationship between the folding conditions and the magnetization of the self-folding microrobots. Folding-invariant magnetization enables the microrobots with imperfect folding shapes to perform predicted rolling motions on a surface. Folding-variant magnetization enables more complex motions to be tuned through shape and magnetization coupling. We demonstrated selective control over the shape of individual microrobots using NIR exposure.

Acknowledgment

Authors would like to thank Prof. Jordi Sort and Jin Zhang for helping us with the VSM measurements, and Dr. Qi Zhang for helping us with computer vision. Financial support by the European Research Council Advanced Grant Microrobotics and Nanomedicine (BOTMED), by the ERC grant agreement n. 247283, and by the Swiss National Science Foundation are gratefully acknowledged.

References

[1] S. Fusco, M. S. Sakar, S. Kennedy, C. Peters, R. Bottani, F. Starsich, *et al.*, "An Integrated Microrobotic Platform for On-Demand, Targeted Therapeutic Interventions," *Adv. Mater.,* vol. 26, pp. 952-957, 2014.

[2] S. Fusco, H.-W. Huang, K. E. Peyer, C. Peters, M. Häberli, A. Ulbers, *et al.*, "Shape-Switching Microrobots for Medical Applications: The Influence of Shape in Drug Delivery and Locomotion," *ACS Appl. Mater. Interfaces,* vol. 7, pp. 6803-6811, 2015/04/01 2015.

[3] M. P. Kummer, J. J. Abbott, B. E. Kratochvil, R. Borer, A. Sengul, and B. J. Nelson, "OctoMag: An Electromagnetic System for 5-DOF Wireless Micromanipulation," *IEEE Trans. Robot.,* vol. 26, pp. 1006-1017, 2010.

[4] S. IPedron, S. van Lierop, P. Horstman, R. Penterman, D. J. Broer, and E. Peeters, "Stimuli Responsive Delivery Vehicles for Cardiac Microtissue Transplantation," *Advanced Functional Materials,* vol. 21, pp. 1624-1630, 2011.

[5] E. Gultepe, J. S. Randhawa, S. Kadam, S. Yamanaka, F. M. Selaru, E. J. Shin, *et al.*, "Biopsy with Thermally-Responsive Untethered Microtools," *Advanced Materials,* vol. 25, pp. 514-519, 2013.

[6] K. Baek, J. H. Jeong, A. Shkumatov, R. Bashir, and H. Kong, "In situ self-folding assembly of a multi-walled hydrogel tube for uniaxial sustained molecular release," *Adv. Mater.,* vol. 25, pp. 5568-73, 2013.

[7] R. Geryak and V. V. Tsukruk, "Reconfigurable and actuating structures from soft materials," *Soft Matter,* vol. 10, pp. 1246-63, Mar 7 2014.

[8] J.-C. Kuo, H.-W. Huang, S.-W. Tung, and Y.-J. Yang, "A hydrogel-based intravascular microgripper manipulated using magnetic fields," *Sensors and Actuators A: Physical,* vol. 211, pp. 121-130, 2014.

[9] S. Timoshenko, "Analysis of bi-metal thermostats.," *J. Opt. Soc. Am. Rev. Sci. Instrum.,* vol. 11, p. 23, 1925.

[10] S. Alben, B. Balakrisnan, and E. Smela, "Edge effects determine the direction of bilayer bending," *Nano Lett.,* vol. 11, pp. 2280-5, Jun 8 2011.

[11] R. Pieters, T. Hsi-Wen, S. Charreyron, D. F. Sargent, and B. J. Nelson, "RodBot: A rolling microrobot for micromanipulation," in *Robotics and Automation (ICRA), 2015 IEEE International Conference on*, 2015, pp. 4042-4047.

[12] M. M. Tirado and J. G. de la Torre, "Translational friction coefficients of rigid, symmetric top macromolecules. Application to circular cylinders," *The Journal of Chemical Physics,* vol. 71, pp. 2581-2587, 1979.

[13] M. M. Tirado and J. G. de la Torre, "Rotational dynamics of rigid, symmetric top macromolecules. Application to circular cylinders," *The Journal of Chemical Physics,* vol. 73, pp. 1986-1993, 1980.

[14] Y. Takaisi, "Note on the Drag on a Circular Cylinder moving with Low Speeds in a Semi-infinite Viscous Liquid bounded by a Plane Wall," *Journal of the Physical Society of Japan,* vol. 11, pp. 1004-1008, 1956/09/15 1956.

[15] S. Champmartin, A. Ambari, and N. Roussel, "Flow around a confined rotating cylinder at small Reynolds number," *Physics of Fluids,* vol. 19, p. 103101, 2007.

[16] C.-H. Zhu, Y. Lu, J.-F. Chen, and S.-H. Yu, "Photothermal Poly(N-isopropylacrylamide)/Fe3O4 Nanocomposite Hydrogel as a Movable Position Heating Source under Remote Control," *Small,* vol. 10, pp. 2796-2800, 2014.

[17] M. A. C. Stuart, W. T. S. Huck, J. Genzer, M. Muller, C. Ober, M. Stamm, *et al.*, "Emerging applications of stimuli-responsive polymer materials," *Nat. Mater.,* vol. 9, pp. 101-113, 2010.